CHARACTERIZATION OF SOLAR-GRADE SILICON PRODUCED BY THE SiF_4-Na PROCESS

by

A. Sanjurjo, K. M. Sancier, R. M. Emerson and S. C. Leach
SRI International, Menlo Park, California 94025
SV423852

J. Minahan
Spectrolab, Sylmar, California 91342
SV839236

ABSTRACT

We have developed a process for producing low-cost solar grade silicon by the reaction between SiF_4 gas and sodium metal. In this paper we present results of the characterization of the silicon. These results include (a) impurity levels, (b) electronic properties of the silicon after crystal growth, and (c) the performance of solar photovoltaic cells fabricated from wafers of the single crystals. The efficiency of the solar cells fabricated from semiconductor silicon and SiF_4-Na silicon was the same.

PRODUCTION AND ANALYSIS OF SILICON

Since the SiF_4-Na process has been described previously,[1,2] it will only be outlined briefly in this section.

The SiF_4-Na process for producing silicon is shown schematically in Figure 1. Briefly, it consists of three major steps: production of SiF_4, production of Si, and recovery of silicon. For the production of SiF_4, NaF is added to an aqueous solution of H_2SiF_6 (a waste product of

the phosphate industry) to precipitate crystalline, nonhygroscopic, Na_2SiF_6. The Na_2SiF_6 is filtered, dried, and thermally decomposed to form SiF_4 gas. The remaining solid residue of NaF is recycled to the precipitation step.

To produce silicon, the SiF_4 gas and sodium are fed continuously to a reactor where they react exothermically to form silicon crystallites dispersed in a matrix of NaF. The silicon is recovered from the product by one of two methods: (a) aqueous leaching of NaF followed by filtration and drying, or (b) melting of both phases to form two immiscible liquids that can be discharged separately. The results presented in this paper pertain only to leached separated silicon.

For convenience we used commercial SiF_4 gas as the source of silicon. We also used commercial sodium without any purification. In most of the production runs, the sodium was fed to a batch reactor as small, solid pieces. In two runs, the sodium was fed as a liquid.

The reactor was operated as follows. For solid sodium feed, the sodium pieces were located in a plastic hopper and fed continuously to the reactor by means of a screw feeder. For liquid sodium feed, the sodium was stored in a stainless steel melter and fed continuously to the reactor by a back pressure of argon gas. The pressure of SiF_4 in the reactor was kept approximately constant at 1 atm by means of a pressure regulator. The temperature of the reactor walls was kept at or above 600°C by means of external heating tapes. This operating temperature was selected to minimize the formation of the byproduct, Na_2SiF_6, by the reaction between SiF_4 and NaF. The reactor vessel was made of Inconel 600 which contained a nickel liner, which in turn was lined with a graphite sheet (Grafoil, Union Carbide Corp.). In a production run we could produce as much as 10 kg of products containing approximately 1.4 kg of silicon and no unreacted sodium. The average production rate was about 0.5 kg of silicon per hour.

During the silicon recovery process, the products from each run were first separated mechanically from the Grafoil liner, crushed to particles smaller than 1 cm in diameter and loaded into the leaching

tanks. Deionized water was used to dissolve the NaF, and H_2SO_4 was added to the initial leach steps to retard silicon oxidation. The slurry of products in the aqueous media was stirred, allowed to settle, and filtered. The leaching process was continued until the fluoride ion concentration was below 10^{-4} M. At that point, silicon powder ranging in size from 1 micron to 1 mm was recovered by vacuum-filtration and dried in a vacuum oven. The recovery yield of silicon powder was typically around 90% with yields as high as 95%. Table 1 shows typical impurities of 14 batches of silicon powder. We used two different SSMS systems, one for Runs A to J, and a second one for runs K to N. High quality semiconductor polycrystalline silicon (10^4 ohm-centimeters) was used to establish the limit of detection of each of the two SSMS systems used for analysis. The operational detection level is shown for each SSMS system in Table 1.

MELT CONSOLIDATION AND CRYSTAL GROWTH

Silicon powder samples were melted in a quartz crucible (7-cm i.d., 13-cm high) under an argon atmosphere. A film of slag was present on the ingots after melt-consolidation. The slag was removed by mechanical grinding and/or by chemical etching in HF or HNO_3-HF mixtures.

Silicon was grown into single crystals by the Czochralski method. A total of eight single crystals were grown from approximately 2 kg of silicon recovered from the melt consolidation steps. Typically 50% to 70% of the melt was pulled as a single crystal. Crystal 6 was grown from remains from the previous crystal growths. All were single crystal except No. 2 which became polycrystalline at 30% growth. The first seven crystals were oriented in the <1,1,1> direction, and the last crystal was oriented in the <1,0,0> direction. The SSMS analysis of two crystals of silicon are shown in columns 2 and 3 of Table 2. The last column shows the SSMS readings for high quality Monsanto semiconductor silicon (10^4 ohm-cm) which was reported to have impurities in the sub-ppm w. level. This high purity silicon was used to determine the limit of detection of the SSMS system. Analysis of carbon and oxygen were made by infrared absorption spectroscopy.

ELECTRONIC CHARACTERIZATION

The electronic characterization of the single crystal wafers produced from the leach-recovered silicon was performed by several techniques and by several laboratories. A summary of the results of resistivity, mobility, and carrier concentration is shown in Table 3.

We measured the resistivity of the wafers from each of the eight single crystals with a four-point probe. For some samples, we used contactless, capacitive probes to verify the values obtained by the four-point probe. Because the agreement among the values obtained by the different techniques was good, only values obtained with the four-point probe are reported in Table 3.

The type of silicon was determined mainly by thermoelectric measurements. The results indicated that all crystals were p-type as shown in Table 3. We checked the results for crystal 1 by making a Si-electrolyte interface and studying its photodiode behavior; the photocurrent measurements confirmed that all crystals were strongly p-type.

We measured the mobility of the carriers in the silicon by using the Hall technique, and the results are shown in Table 3.

Carrier concentration was estimated by making a silicon wafer electrode in an electrolytic solution and studying the capacity that could be developed in the silicon by applying a potential across the silicon/electrolyte interface. The silicon wafer was polished and etched to diminish the density of surface states due to mechanical damage. Thus, the capacitance measured was essentially equal to the capacitance in the bulk (space charge region) of the semiconductor.

The voltage dependence of the space-charge capacitance of the semiconductor at the electrolyte/semiconductor interface was plotted according to the Mott-Schottky relationship for a p-type semiconductor

$$1/C^2 = \frac{2}{qN_A E E_0} (- V + V_{fb} - kT/q)$$

In this equation, q is the charge of the electron, N_A is the acceptor density, C and Co are the dielectric constants in the semiconductor and in vacuum, respectively, V is the applied potential, and V_{fb} is the flatband potential. From the sign of the slope of this equation, we can determine the conductivity type of the material. We confirmed in this way that our silicon is a p-type semiconductor. From the magnitude of the slope, we calcualted N_A, the acceptor density, to be 3.9×10^{-16} reciprocal centimeters for a wafer from crystal 1. The carrier concentrations for all other crystals were obtained from resistivity and mobility values determined by the standard Hall technique.

The carrier lifetime (t) was determined with a Loe instrument from photocapacitance decay curves. In this technique a Xe laser pulse hits the surface of the wafer and produces an increase in electron-hole pairs that immediately start to recombine to reestablish equilibrium. The temporary increment in carrier concentration results in an increase in conductivity that can be detected by the change in intensity of the reflection of microwaves on the silicon wafer. The lifetime was determined by following the decay in conductivity with time after the light pulse. The silicon wafers were used as-cut, without any polishing to diminish surface states. Therefore, the measured lifetime values reported here may be smaller than that of intrinsic bulk lifetimes.

Another technique for measuring very low concentrations of impurities is deep level transient spectroscopy. Measurements were performed in this technique on wafers from crystal 1 by Dr. P. Claus et al. of the University of Ghent in Belgium. There were no detectable traces of transition metal contamination.

SOLAR CELL FABRICATION AND CHARACTERIZATION

The following procedure was used to prepare the silicon wafer for fabrication as solar cells and subsequent characterization of the cells. A number of 2-inch diameter control wafers of high quality semiconductor silicon (1-3 ohm-cm) were included with the fabrication lot. Wafers were cleaned and then etched to a thickness of ~ 0.025 cm. This was expected to remove mechanical damage that might have arisen from slicing the wafers. Following rigorous surface cleaning, the wafers were placed in a quartz boat and inserted into a clean quartz tube within a furnace at 825°C. The wafers were subjected to a 5-minute warmup in a nitrogen/oxygen atmosphere; to phosphorous deposition for 3 minutes in a mixture of nitrogen, oxygen, and phosphine; and to a 5-minute "drive" in nitrogen.

After removing the wafers from the diffusion furnace, resistivity (V/I) measurements were made using a four-point probe.

The front of the wafers were masked with ink, dried, and then etched in a 60:40 solution of HNO_3:HF for 5-8 seconds to remove the n^+ type layer from the base. A dicing saw was used to cut the wafers into 2-cm squares. All cells were cleaned, and then mounted in evaporation masks and metallized, front and back, with an electron gun evaporation system. Titanium, palladium, and silver were deposited, in that order, on the front of the wafers with layer thicknesses of 800A, 400A, and ~ 50,000A, respectively. Aluminum, titanium, palladium, and silver were deposited in that order on the back of the wafers. The 2 cm x 2 cm metallized solar cells were then mounted in masks and placed in an electron beam evaporator. Dual anti-reflecting films of TiO_2 and Al_2O_3 were deposited on the front surface. Wafer edges were then etched, after masking front and back, to remove any inadvertently-deposited metals from the cell edges. The contact metallization system used on each cell occupied 0.172 cm^2 of the cell front area. Each of the 20 grid lines were 0.0033 cm in width, while the ohmic bars and contact tables occupied 0.032 cm^2. Front metallization thickness was approximately 0.0006 cm.

The solar cells were characterized as follows. Illuminated I-V measurements were made using a Spectrolab X-25 Solar Simulator. Spectral response was measured using a 14 segment filter wheel assembly. Measurements of resistivity, V/I, and dark current were made using conventional volt meters and power supplies. The maximum power point was measured from the I-V curve using standard power curves. Fill factor, FF and efficiency, EFF were calculated using

$$EFF = \frac{P_{max}(mW)}{135.3\ mW/cm^2 \times 4\ cm^2}$$

$$FF = \frac{I_{max} \times V_{max}}{I_{sc} \times V_{oc}}$$

The results of the characterization of the solar cells are shown in Table 4 for the open circuit potential (VOC), short circuit current (ISC), maximum power (PMX), fill factor (FF), and efficiency (EFF) at AMO. In the last column is shown the value of the efficiency at AM1 which was calculated by multiplying the value of AMO by the factor 1.14 (10). The SiF_4-Na cells examined were made from wafers cut from four crystals: 3, 5, 7, and 8, with the slice number (starting from the seed end) following the hyphen. The eight cells made from semiconductor silicon are indicated by a prefix C. The low efficiency of cell 7-11 resulted from a shunting problem that occurred during manufacture.

The overall results indicate that solar cells made from SiF_4-Na silicon have efficiencies equal to those made from semiconductor grade silicon in the same batch.

DISCUSSION

It is possible presently to use the impurity content in silicon to predict the suitability of polycrystalline silicon for the manufacture of single crystal solar cells. The work by Hill at Monsanto[4] and of

Hopkins et al.[5] and Davis et al.[6] at Westinghouse resulted in the establishment of maximum levels that can be permitted for each impurity in silicon without affecting the efficiency of solar cell manufactured from that silicon. The work done by Pizzini[7] and Galluzi et al.[8], among others, has also started to establish the same type of levels for polycrystalline silicon solar cells. These definitions cannot be taken as absolute guidelines as pointed out by the authors above because the efficiency of the solar cells also depends on the type of crystal growth and the cell manufacturing process. Nevertheless, these impurity values (such as in Table 5) can be used as general guidelines. Therefore, the first test of the suitability of our silicon for solar cell manufacture was to analyze it. Because the maximum allowable impurity levels in solar grade silicon (Sol-Si), as established by the authors mentioned above, are roughly at the low ppm w. level, only techniques such as Spark Source Mass Spectrometry (SSMS) can be used. Even when using the SSMS technique, some precautions have to be taken in order to obtain reliable analyses. Some of the typical sources of error in the SSMS values include common sampling errors, inhomogeneity of the sample, and SSMS system background shifts or contamination. We determined first the limits of detection of the SSMS systems by analyzing very high purity Monsanto polycrystalline semiconductor silicon (10,000 ohm cm). We use these readings to define the limit of detection for each impurity. We also determine the reliability of the readings by analyzing the same sample in different days. We concluded that the reproducibility of the readings was not perfect, but most of the readings for each impurity were within a factor of 2 from the average. This finding is similar to that reported by Hunt et al.[9] The sampling errors and inhomogeneity of the sample were less of a problem. In our case, the silicon is in the form of powder with an average particle size of 100 microns. The samples were taken using normal sampling techniques and we believe, therefore, that they were representative of each batch.

Taking the preceding remarks into account, we can interpret the values in Table 1 (runs I to J) as indicating that all the silicon batches were very pure and they all had similar composition. This

result is of great industrial importance because it gives assurances that the purity of silicon produced by the SiF_4-Na process will be constant. In addition, because the readings were so close to the limit of detection, we suspected that the silicon might be purer than those readings indicate. In effect, when a different SSMS system (System 2 in Table 1, runs K to L) with higher sensitivity was used, the readings for some of the impurities were lower, although the silicon had been produced in basically the same conditions as before. In particular, Ti readings were a few ppm.w in System 1, but they were below 200 ppb.w in batches analyzed with System 2. Phosphorous readings were also lower with System 2. Later, we determined that all the silicon is strongly p-type, without any sign of compensation and has a resistivity of 0.3 to 5 ohm cm which indicate P levels much lower than those indicated by the SSMS readings. In Table 5, we compare the readings in System 2 with the definition of solar grade as proposed by Hopkins et al. It is clear that the SiF_4-Na silicon is much purer than required for solar cell manufacture. The only possible exception is Na, but as we describe below, this impurity can be removed almost completely.

The melt consolidation and crystal growth step result, as expected, in great purification, as can be seen by comparing the values in Tables 1 and 2. The level of Na, which is typically at the 10^2 ppm w level in the silicon powder, is below detection limit in the polycrystalline ingot and, naturally, in the final silicon crystal. In independent mass spectrometric studies we have observed that Na in silicon starts vaporizing at 600°C and the volatilization becomes very fast at temperatures above 1000°C. The low initial levels of the transition metals in the silicon powder, combined with the normal purification during crystal growth, should result in values at the sub ppb w levels. In effect, Deep Level Transient Spectroscopy studies of the silicon wafers from crystal 2 did not show any indication of the existence of transition metals. The limit of detection for this technique ranges from 10^{12} to 10^{14} atoms per cm^3. Therefore, the readings for the transition metals in Table 2 for crystals 1 and 2 are again indicative of the limit of detection of the SSMS system. These

readings and those for the semiconductor silicon also illustrate the typical variability of the limit of detection of the SSMS system for three extra pure but different samples.

The variations in the values of the electronic parameters are not well understood yet (more studies are in progress), but they were well within the range expected for crystals grown from different melts, obtained from the mixture of powders from different production batches. When the crystals were grown from exactly the same melt as was the case for crystals 3 and 4, their characteristics were reasonably similar. Crystal 6 was grown from remains of previous crystal growths. Its higher resistivity and lower mobility may be due to high content of C.

The photovoltaic behavior of the silicon was studied in several laboratories, and solar cells were manufactured in experimental and in industrial lines. The results were consistently indicative of high performance indistinguishable from that of cells made from semiconductor silicon. Although all crystals (except No. 2) were investigated, only the results of crystals 3, 5, 7 and 8 are shown here. The efficiency values were determined in AM0 conditions. Based on results obtained at Spectrolab[11] and elsewhere, we know that the efficiency at AM1 can be estimated by multiplying the AM0 efficiency by a factor which ranges in value from 1.14 to 1.18. Taking the conservative approach, we used the 1.14 value in this work to estimate the AM1 values shown in Table 4.

A comparison of control cell and experimental cell efficiencies would indicate that the better lifetime to be found in the semiconductor silicon has resulted in a somewhat better short circuit current characteristic, especially in the case of the lower resistivity material. This shortcoming is balanced however by the higher open circuit voltage that one expects from lower resistivity base material. Efficiency can be enhanced by means of front surface texturing [(100) only] and by introduction of a back surface field on the higher resistivity material. A back surface field effect will be more obvious on higher lifetime material. Some examples of these effects are shown in Table 6.

CONCLUSIONS

Silicon produced from commercial SiF_4 and Na is more than pure enough to be used in the fabrication of solar cells of high efficiency. All the results obtained--chemical analysis, electronic parameters, cell efficiencies--demonstrate clearly the high quality of the SiF_4-Na silicon.

The fact that the quality of the silicon was consistently high in all batches indicates clearly that the process can be scaled up with confidence to the industrial scale. This process produces silicon of much higher purity than any of the processes developed for solar cell manufacture based on the direct purification of metallurgical grade silicon, and at a projected cost much lower than the projected costs for halosilane-based processes. Therefore, it holds great promise for decreasing the overall cost of silicon solar cells.

ACKNOWLEDGEMENTS

We wish to thank Dr. W. Allred of Crystal Specialties, Inc. and Mr. R. May of Aerojet General Corp. for growing the single crystal. We also wish to thank our colleagues, Drs. P. Jorgensen and D. Hildenbrand and Mr. J. Harsch, for their advice and support of the program, as well as Dr. Marc Madou for this electronic characterization, and Mssrs. George Craig and Mike Gusman for their technical support. We also wish to express gratitude to our colleagues Dr. G. Marchetti of Enichimica; Drs. G. Missoni, G. Sironi, F. Galluzzi and E. Scaffe of Eniricerche (Italy) for their advice and comments.

REFERENCES

1. A. Sanjurjo et al., J. Electrochem. Soc. 128(1), 79 (1981).

2. A. Sanjurjo and K. Sancier, "Silicon Material Preparation and Economical Wafering Methods," R. Lutwack and A. Morrison, E. Noyes, Publishers, New Jersey, U.S.A. (1984).

3. Marc Madou, "Bulk and Surface Characterization of Silicon," Surface Science, Vol. 108, pp. 135-152 (1981).

4. D. E. Hill et al. Final Report, "Determination of a Definition of Solar Grade Silicon," ERDA/JPL RA54-338-76 (1976).

5. R. Hopkins et al., Final Report, "Effect of Impurities and Processing on Silicon Solar Cells," DOE/JPL 954-331-81/14 (1982).

6. S. R. Davis et al., IEEE Trans. of Elect. Devices, ED-27, 677 (1980).

7. S. Pizzini et al., "Materials and New Processing Technologies for Photovoltaics," Ed. J. Amick, V. Kapur. S. Dietl, Proc. J. Elect. Soc. 83(11), 200-220 (1983).

8. F. Galluzi et al., Extend. Abst., J. Electrochem. Soc. 84(2), Abst. No. 340 (1984).

9. L. Hunt et al, Extend. Abst., J. Electrochem. Soc.

10. G. F. J. Garlick, Private Communication.

11. J. A. Minahan et al., "Solar Cells Fabricated with Unconventional Silicon Materials", Proceedings IEEE 15th Photovoltaic Specialists Conference, Orlando, FL. (1981) p. 608.

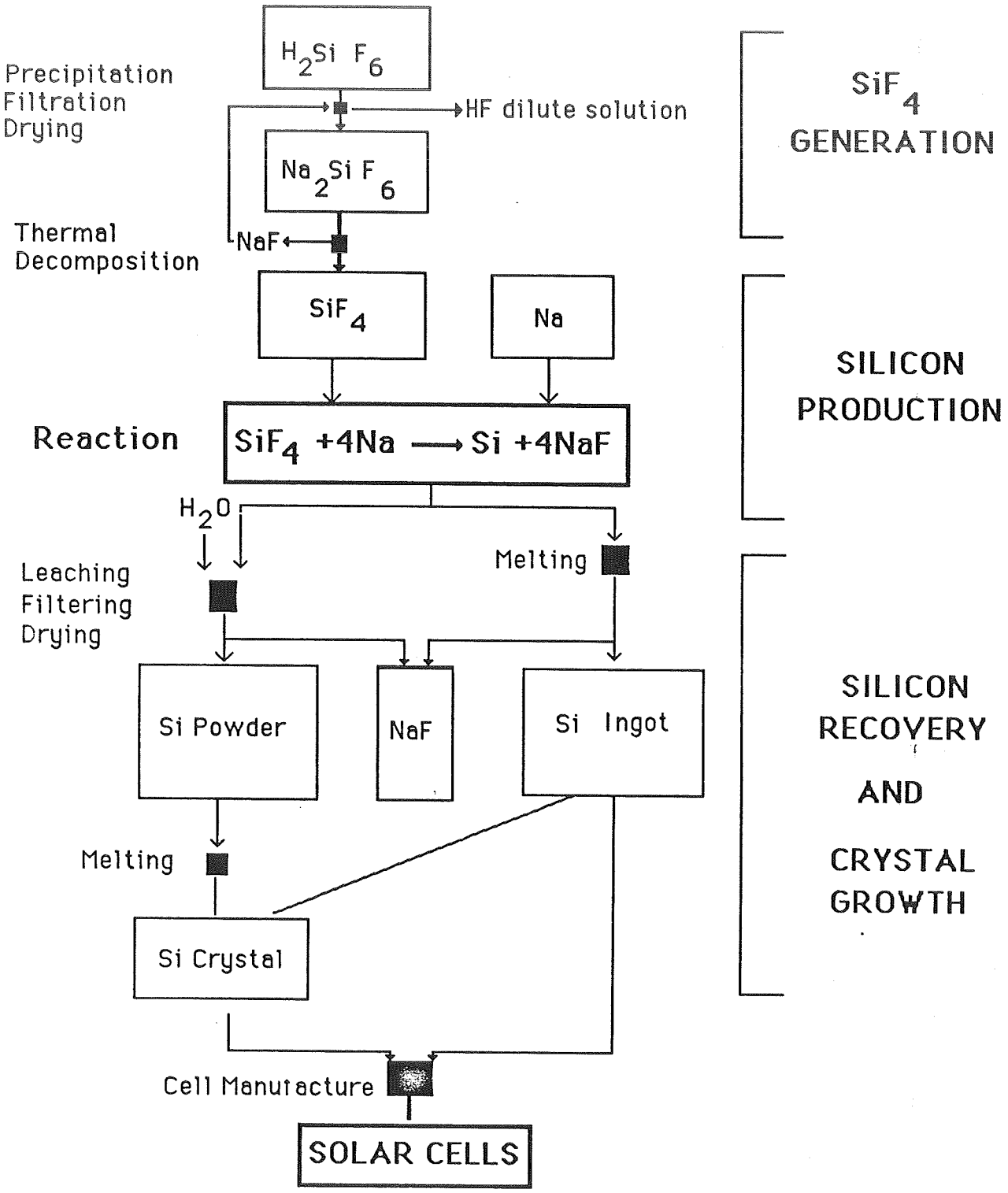

FIGURE 1. Schematic of the SiF4 - Na Process

Table 1

SPARK SOURCE MASS SPECTROMETRY ANALYSES OF LEACH-RECOVERED Si POWDER (ppm, w.)

	SSMS SYSTEM 1											SSMS SYSTEM 2				
Impurity	A	B	C	D	E	F	G	H	I	J	Limit of Detection	K	L	M	N	Limit of Detection
B	0.2	0.1	<0.1	0.2	<0.1	0.1	<0.1	<1	<0.1	<0.1	<0.1	0.2	0.2	0.04	0.02	0.02
Al	0.8	0.4	0.4	2	0.4	3	1	0.1	0.3	0.2	0.4	2	0.2	0.1	0.1	0.2
P	1	2	2	4	0.7	0.2	0.1	1	1	0.6	0.3	0.2	0.1	0.05	0.03	0.05
As	0.6	2	2	0.3	4	1	1	2	3	1	<0.3	<0.3	<0.3	<0.3	<0.3	<0.03
Ti	3	1	1	2	6	2	0.3	7	4	4	0.2	<0.2	<0.2	<0.2	<0.2	<0.08
Zr	<0.1	0.1	<0.3	<0.4	0.5	<0.3	0.1	0.3	0.4	0.7	<0.3	<0.3	<0.3	<0.3	<0.3	<0.1
V	<0.1	0.1	<0.1	0.1	0.1	<0.1	<0.1	0.1	<0.1	<0.1	<0.3	<0.2	<0.2	<0.2	<0.2	<0.08
Ta	0.4	--	<0.1	0.8	<0.1	<0.1	<0.1	<0.1	<0.1	<0.1		<0.7	<0.7	<0.7	<0.7	<0.2
Cr	1	4	4	<6	<1	2	3	11	11	13	<0.3	0.7	<0.4	<0.4	<0.4	0.1
Mo	<0.6	1	1	2	0.9	1	0.7	1	1	0.7	<0.3	<0.3	<0.3	<0.3	<0.3	<0.1
W	<0.1	--	<0.1	<0.1	<0.1	<0.1	<0.1	<0.1	<0.1	<0.1		<0.7	<0.7	<0.7	<0.7	0.2
Mn	0.3	0.1	<0.1	0.1	0.7	0.7	0.1	0.5	0.2	0.1	<0.3	0.1	0.04	0.04	0.04	0.05
Fe	--	--	--	--	--	--	--	--	--	--	<0.3	<2	<2	<2	<2	<0.4
Co	--	--	--	--	--	--	--	--	--	--	0.5	<0.2	<0.2	<0.2	<0.2	0.1
Ni	--	--	--	--	--	--	--	--	--	--	4	<0.4	<0.4	<0.4	<0.4	<0.2
Cu	0.9	--	0.9	0.5	2	1	0.7	3	2	0.8	0.2	0.5	0.07	0.05	0.03	0.2
Zn	4	--	3	1	1	6	0.7	0.9	1	1	15	<0.2	<0.2	<0.2	<0.2	<0.3
Na	<160	230	<230	<370	<480	<330	<160	<340	160	<390	9	<300	<100	3	2	1
K	17	--	14	9	23	36	96	4	20	12	0.1	3	3	0.8	0.8	1
Mg	3	9	9	6	2	14	3	6	2	3	<0.3	2	<1	<1	<1	0.1
Ca											0.1		15	3	3	1
Ba	<0.5	--	<0.4	4	<5	0.3	<1	1	<0.1	<0.1	--	<0.5	<0.5	<0.5	<0.5	<0.5
S	5	2	2	3	20	7	7	3	5	21	--	<0.1	<0.1	<0.1	<0.1	--

Table 2

SSMS ANALYSIS OF SRI SILICON CRYSTALS AND SEMICONDUCTOR REFERENCE
(ppmw)

Impurity	SRI Si CRYSTAL 1	SRI Si CRYSTAL 2	Semiconductor Si
B	0.02	0.08	0.02
Al	0.3	0.2	0.2
P	0.03	0.1	0.05
As	⩽ 0.03	< 0.05	⩽ 0.03
Ti	< 0.08	< 0.1	< 0.08
Zr	< 0.1	< 0.1	⩽ 0.1
V	< 0.08	< 0.1	< 0.008
Ta	< 0.3	--	< 0.2
Cr	< 0.08	0.04	0.1
Mo	< 0.2	--	< 0.1
W			< 0.2
Mn	0.02	--	0.05
Fe	< 0.4	2	< 0.4
Co	< 0.2	< 0.2	< 0.1
Ni	< 0.2	< 0.2	< 0.2
Cu	0.2	0.02	0.2
Zn		< 0.08	< 0.3
Na			1
K	--	--	1
Mg	0.05	0.05	0.1
Ca	0.07	0.1	1
Ba	--	--	< 0.5
C	6-10	5*	1*
O	12	10*	10*

*Infrared Absorption Nicolet Spectrometer

Table 3

CRYSTALLOGRAPHIC AND ELECTRONIC PARAMETERS

Parameter	Crystal 1	2	3	4	5	6	7	8
Orientation	<111>	<111>	<111>	<111>	<111>	<111>	<111>	<100>
Resistivity ρ(Ω cm)i	0.5 ± 0.05	2	0.6 ± 0.2	0.65 ± 0.05	0.6 ± 0.1	1.3 ± 0.05	2 ± 0.2	0.35 ± 0.(
Type	p	p	p	p	p	p	p	p
Mobility ($cm^2/V\ s$)i	310-320	--	--	278	215	-82	184	203-303
Carrier concentration (atoms/cm^3)	3.9×10^{16}	--	--	3.6×10^{16}	4.8×10^{16}	7.5×10^{16}	2.25×10^{16}	9.9-5.7 x
Carrier lifetime (μs)	5-14	3.						
Diffusion Length			120-150	80-130	100-110	100-130	100-150	120-150

Table 4

SOLAR CELL CHARACTERISTICS

		VOC (MV)	ISC[a] (MA)	PMX (MW)	CFF	EFF(AMO) %	EFF(AM1)[b] %
	C-3	603	150	67.9	.750	12.5	14.3
	C-17a	592	154	72.9	.799	13.5	15.4
	C-17b	591	155	72.0	.786	13.3	15.2
Control	C-18a	591	153	69.7	.771	12.9	14.7
Cells	C-18b	589	155	69.4	.761	12.9	14.6
(Semi-	C-19	585	153	71.5	.799	13.2	15.0
Si)	C-20a	591	154	71.6	.787	13.2	15.0
	C-20b	586	153	66.7	.744	12.3	14.0
	3-B	615	153	73.4	.780	13.6	15.5
	5-30	600	145	67.0	.770	12.4	14.1
	5-24	596	148	67.0	.759	12.4	14.1
	5-85	607	149	71.4	.789	13.2	15.1
Sample	5-12	608	149	71.0	.784	13.1	14.9
Cells	5-42	608	150	72.1	.790	13.3	15.2
(SRI-Si)	7-11	222	143	15.4	.485	2.8	--
	7-63	585	153	67.7	.757	12.5	14.3
	7-57	576	152	67.6	.770	12.5	14.3
	8-26	615	150	67.7	.734	12.5	14.3

[a]2 x 2 cm cells.

[b]EFF(AM1) estimated from AMO. Multiplying factor 1.14.

Table 5

IMPURITY THRESHOLD LEVELS FOR SOLAR GRADE Si

VERSUS

IMPURITY LEVELS IN Si PRODUCED BY THE SiF_4-Na PROCESS

	Impurity Threshold Levels		
Element	100% Max Efficiency[a]	90% Max Efficiency[b]	Si from SiF_4-Na
Al	0.4	0.7	0.1-0.2
Ti	0.9	4.5	< 0.2
Zr	10.5	325	< 0.3
V	0.6	4	< 0.2
Ta	--	90	
Cr	16	133	< 0.4-0.7
Mo	--	65	< 0.3
W	--	1000	< 0.7
Mn	16	150	0.04-0.1
Fe	32	372	< 2
Co	10	194	< 0.2
Ni	17	--	< 0.4
Cu	280	4500	0.03-0.5

(a) Maximum impurity level allowed in polycrystalline silicon feedstock that does not result in degradation of single crystal solar cells manufactured from that silicon.

(b) Impurity level that results in single crystal cells with only efficiencies of 90% of those produced with ultrapure semiconductor Si.

Table 6

EFFECTS ON CELL EFFICIENCY OF BACK SURFACE FIELD, AND TEXTURE

Cell No.	V_{oc}	I_{sc}	FF	η(AMO)	Projected η(AMO)
C-1**	585	173	.639	12.0	15.0
C-5a*	612	164	.779	14.4	14.8
3-B	615	153	.780	13.6	13.9
C-17a	592	154	.779	13.5	13.5
7-10*	593	159	.655	11.4	13.9
7-63	585	153	.757	12.5	13.2
8-28*	602	150	.692	11.5	13.3
8-26	615	150	.734	12.5	13.6

*Back surface field.

**Back surface field, front textured cell.

Note: The projected efficiency at AMO is the efficiency that cell would have had if its fill factor were .799, the value for Cell C-17a.

omit

DISCUSSION

SCHWUTTKE: I congratulate you on your semiconductor-grade silicon. I assume that you have used this material to make solar cells. What kind of cell efficiency did you obtain using this type of material?

SANJURJO: You mean the last material? No, we haven't.

SCHWUTTKE: Oh, that's too bad.

SANJURJO: Well, I think so, but basically our program has been switched to preparing semiconductor-grade silicon.

SCHWUTTKE: I think it would be extremely interesting to determine cell efficiencies using this material.

SANJURJO: Every time we made solar cells with the previous material, we had the possibility of getting even higher efficiencies and we were limited by several things. One was the saw damage, which was not properly etched. There were some problems in the fabrication itself so that when we tried to use back-surface fields, we had very scattered data with shunting of several of the cells, including the control cells. Therefore, we were limited to a certain extent. We could have probably obtained high efficiency for both the semiconductor-grade and solar-grade cells. One thing that we would like to do is to get the highest purity material we can, and try to make the best solar cells and then compare it with our product.

SCHWUTTKE: Looking at the cell data of the Spectrolab labs and cells from your solar-grade material, the efficiencies are very similar. Are the areas for the cells the same?

SANJURJO: The same. All of these cells were 2 x 2 cm cells, and they were co-processed and intermixed.

SCHWUTTKE: Did Spectrolab use a standard baseline process or a high-efficiency process?

SANJURJO: For their level, I think it was a standard process.

SCHWUTTKE: Do the cells have a back-surface field?

SANJURJO: No. The cells were without back-surface field. Then we tried with the back-surface field. The particular batch used had several short-circuited cells. The aluminum somehow got through on both batches of the semiconductor grade and on our material. I have some information in the paper regarding the effect of back-surface fields. The major effect was probably in the semiconductor silicon cells which had a diffusion length of about 180 μm and higher. Our best cells were about 150 to 180 μm, and some of the others were 100 to 150 μm.

omit

SCHWUTTKE: What was the cell thickness: 150 or 200 μm?

SANJURJO: We used 300 to 500 μm. The cells were made not only by Spectrolab, but also by two other laboratories, one of which used an industrial-cell fabrication line. The efficiencies of the reference semiconductor cells were always the same, but the cells from the industrial line had lower efficiencies. The nominal average for both semiconductor and our cells was 12.5% AM1.

LEIPOLD: I noticed that the open-circuit voltage for the cells made from your material was higher. Were they the same base resistivities? Do you have an explanation?

SANJURJO: There was a slight difference. Our cells had higher open circuit voltage, and the semiconductor cells had higher short-circuit current. There is some information relative to this in the paper, but more work is needed to characterize the material. We felt that the crystals were very good for the first attempt, but better crystals are required. We were limited by the crystals and by the processing of the wafers to a point that we did not make any determination with respect to any other differences. The differences are probably due to the crystal growth rather than the material.